GEOPHYSICAL RESEARCH LETTERS, VOL. 23, NO. 25, PAGES 3679-3682, DECEMBER 15, 1996

Magnetopause transects

B.U.Ö. Sonnerup and M. Guo

Thayer School of Engineering, Dartmouth College, Hanover, NH

Abstract. A novel method is described for reconstruction of two-dimensional current-layer structures from measurements taken by a single spacecraft traversing the layer. In its present form, the method is applicable only to 2D magneto-hydrostatic structures that are passively convected past the observing spacecraft. It is tested on a magnetopause crossing of the tangential-discontinuity type by the spacecraft AMPTE/IRM. The magnetic structures recovered include a magnetic island located between two X-type nulls as well as a magnetic 'worm hole' through which a bundle of weak magnetic flux appears to connect the magnetosphere and the magnetosheath.

Introduction

Obtaining observational information about the structure of the magnetopause current layer has been of high interest since the early sixties. In most studies to date [e.g., *Sonnerup et al.*, 1990], plasma and magnetic field observations during a magnetopause crossing were compared to two simple one-dimensional (1D) models of the current-layer structure: for magnetic-field reconnection events a so-called rotational discontinuity (RD) in which the normal magnetic field component, B_n, is locally non-zero and in which associated Alfvénic plasma flow across the magnetopause and jetting along it occurs; for non-reconnection events a so-called tangential discontinuity (TD) in which no dynamically significant B_n is locally present and no jetting occurs.

In the present article we briefly describe, and test by use of AMPTE/IRM data, a method for reconstructing 2D coherent magnetic-field structures within the magnetopause itself from single-spacecraft data, collected as these structures move past the observation platform. In its present form the method is restricted to structures of the TD type, e.g., a current layer with embedded tearing-mode islands, but it can be extended in principle to describe RDs as well.

Method

The basic assumptions of our model are: (i) that a set of 2D magnetic/plasma structures convect past an observing space-craft; (ii) that these structures do not change their configuration significantly during the time interval used in the analysis; (iii) that the plasma velocity observed in a frame moving with the structure is small compared to the local Alfvén and sound speeds so that inertia effects are negligible. The moving frame could be a so-called deHoffmann-Teller (HT) frame in which the entire electric field vanishes, although the existence of an HT frame is an overly restrictive requirement: it suffices that the electric field component in the invariant direction vanishes in the frame moving with the structure.

Paper number 96GL03573.
0094-8534/96/96GL-03573$05.00

In the moving frame, the equilibrium is then a magnetohydrostatic one in which magnetic forces are balanced by pressure forces:

$$\nabla p = \mathbf{j} \times \mathbf{B}. \tag{1}$$

For 2D structures with invariance along the z axis, say, this equation is known to reduce to the Grad-Shafranov (GS) equation (e.g., *Sturrock*, 1994)

$$\nabla^2 A = -\mu_o j_z = -\mu_o \, d(p + B_z^2/2\mu_o)/dA \tag{2}$$

where A(x,y) is the one-dimensional vector potential describing the transverse field, i.e.,

$$\mathbf{B} = (B_x, B_y, B_z) = (\partial A/\partial y, -\partial A/\partial x, B_z(x,y)) \tag{3}$$

and where the pressure $p = p(A)$ and $B_z = B_z(A)$.

In a frame moving with the structure in the xy plane, we assume the spacecraft to traverse it with constant velocity $\mathbf{v}_o$ along a slanted trajectory, as shown schematically in Fig. 1. We let the x axis be along this trajectory and the y axis perpendicular to it, as shown in the figure, so that $\mathbf{v}_o = v_{ox}\hat{\mathbf{x}}$. Since the structure is assumed time stationary, the spacecraft then observes a time rate of change of A given by

$$dA/dt = \mathbf{v}_o \cdot \nabla A = v_{ox} \, \partial A/\partial x = -v_{ox} B_y(t) \tag{4}$$

where $B_y(t)$ is known from the spacecraft magnetometer data. This expression can be integrated to give

$$A(t) = -v_{ox} \int_o^t B_y(\tilde{t}) \, d\tilde{t} \tag{5}$$

Finally, with $x = v_{ox}t$ and $\Delta x = v_{ox}\Delta t$, the discrete version of formula (5) can be used to find A(x) at points separated by distances Δx along the trajectory.

Since p and B_z are measured at a set of points along the trajectory, and since the A value is now known at each of these points, one may test whether $(p + B_z^2/2\mu_o)$, or p and B_z separately, are indeed functions of A alone. In principle, the invariant (z) axis, which is tangential to the magnetopause, can be found by rotating it in small angular steps around the magnetopause normal vector, **n**, calculating A(x) from (5) and then plotting $(p + B_z^2/2\mu_o)$ as a function of A at each step until an optimal correlation is found. Note that the functional relationship between $(p + B_z^2/2\mu_o)$ and A can have more than one branch: the theory of 2D magnetostatic equilibria only requires $(p + B_z^2/2\mu_o)$ (as well as p and B_z separately) to have the same value along each field line but not necessarily on two different field lines having the same A value.

Assuming that the invariant axis is known, either from the method described above or from multi-spacecraft data, and that

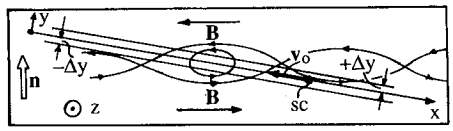

Figure 1. Schematic of spacecraft trajectory through magnetopause structures.

the function A(x) has been determined from (5) at points along the spacecraft trajectory, we may now integrate the GS equation by moving away from the trajectory in small steps, $\pm\Delta y$, as illustrated in Fig.1. The problem is of the Cauchy type with A(x), and therefore $\partial A/\partial x = -B_y$ and $\partial^2 A/\partial x^2$, known on the trajectory, along with $\partial A/\partial y = B_x$ and $(p+B_z^2/2\mu_o)$. In general, we may write the Taylor expansion

$$A(x,y\pm\Delta y) \simeq A(x,y) \pm \partial A/\partial y \Delta y + \frac{1}{2}\partial^2 A/\partial y^2 (\Delta y)^2 \qquad (6)$$

where the second derivative can be evaluated from (2):

$$\partial^2 A/\partial y^2 = -\partial^2 A/\partial x^2 - \mu_o d(p+B_z^2/2\mu_o)/dA\ . \qquad (7)$$

At each step, $\pm\Delta y$, in the integration process, one grid point is lost at each end of the data interval: if data are given at N grid points along the trajectory, (N-2) points will remain at $y = \pm\Delta y$, (N-4) points at $y = \pm 2\Delta y$, etc. Thus the domain in which the vector potential can be calculated is a rhombus with the spacecraft trajectory along one diagonal and with aspect ratio $\Delta y/\Delta x$. Further, the distance along $\pm y$ that the integration gives unique results may be limited by the appearance of field lines not encountered by the spacecraft.

A numerical GS solver of the type described above has been developed and successfully benchmarked against the exact analytical solution, $A = \ln[\cos x + \sqrt{2}\ \cosh y]$, of the GS equation $\nabla^2 A = \exp(-2A)$, describing a current layer containing a string of large-amplitude tearing-mode islands.

Application

To demonstrate the feasibility of our method, we have applied it to an AMPTE/IRM magnetopause crossing on October 19, 1984, 05:18:20-05:19:26 UT. This crossing, which occurred at 9.8 R_E, 9.35 h local time, and 18.5° GSE north latitude was the last in a series of nine magnetopause traversals during an outbound pass of the spacecraft [*Paschmann et al.* 1986]. It was preceded by a low-latitude boundary layer lasting about 5 min. The crossing was analyzed in detail by *Sonnerup et al.* [1990], using magnetic data averaged over a spin period (4.35s) of the spacecraft and corresponding to the plasma sampling interval. It was found to have the following properties:

(i) A high-quality normal vector was obtained from minimum-variance analysis of the **B**-field data. The resulting average normal magnetic field component $\langle\mathbf{B}\rangle\bullet\mathbf{n} = B_n = -0.6$ nT, as shown in the right-hand magnetic hodogram in Fig. 2 (in which B_k represents B_n), which is consistent with $B_n = 0$ within error bounds. This normal (GSE:0.8668, –0.4982, 0.0198) was also close to that found from maximum variance analysis of the convection electric field, $\mathbf{E}_c = -\mathbf{v}\times\mathbf{B}$, and it was within a few degrees of Fairfield's model normal. In a 1D current-layer model, the net magnetopause current would be approximately along the negative intermediate variance axis (–**j** in Fig. 2) with magnitude $I \cong 84$ A/km.

(ii) A good HT frame existed in which the residual electric field was small. The correlation coefficient between the individual X,Y,Z (GSE) components of $\mathbf{E}_c$ and the corresponding components of $\mathbf{E}_{HT} = -\mathbf{v}_{HT}\times\mathbf{B}$ was 0.994 with $\mathbf{v}_{HT}$ = (GSE:–123, –223, 75) km/s. A modified version, $\tilde{\mathbf{v}}_{HT}$, of this velocity, projected onto the xy plane, will play the role of the negative of the spacecraft velocity $\mathbf{v}_o$ through the structure, i.e., $v_o = -\tilde{v}_{HTx}$.

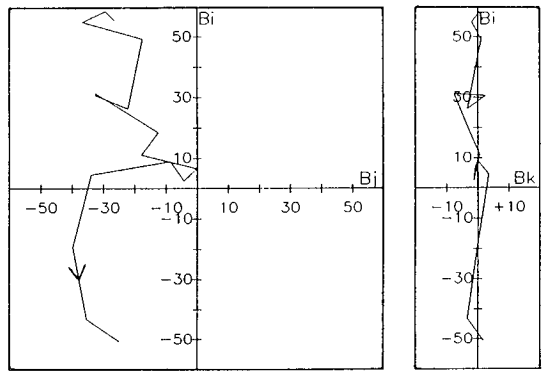

Figure 2. Magnetic hodogram pair for magnetopause crossing by AMPTE/IRM on October 19, 1984, 05:18:20 - 05:19:26 UT. Normal direction is denoted by subscript k. The –z axis corresponds to subscript j. Eigenvalues (nT^2) and eigenvectors in GSE, and in the order (**i**, **j**, **k**), are: $1012nT^2$ (–.4071,–.6843,.6049); $138nT^2$ (–.2878,–.5324,–.7960); $7nT^2$ (.8668,–.4982,.0198) [*Sonnerup et al.*, 1990].

(iii) The residual plasma velocities in the HT frame were of the order of 50 km/s which is much less than the local Alfvén and sound speeds (250-300 km/s).

The magnetopause structure for this event would seem to be a clear case of a TD containing 2D or perhaps 3D internal structures which convect past AMPTE/IRM approximately with the plasma velocity and which cause the normal magnetic field component to fluctuate around zero as shown on the right in Fig. 2. However, there are two inconsistencies in the results derived from the observations.

First, the normal magnetopause velocity $\mathbf{v}_{HT}\bullet\mathbf{n} = +6$ km/s whereas a negative value of this velocity is required in order for the spacecraft to move across the magnetopause in the observed direction (from the magnetosphere to the magnetosheath). In view of uncertainties in the determination of **n** and $\mathbf{v}_{HT}$ this discrepancy is not significant. However, it is evident from (5) that, via B_y, the field map to be generated will be sensitive to the orientation of the y axis and thus also to the x axis which is along the component of the true HT velocity perpendicular to the invariant (z) direction (i.e., $v_{HTy} = 0$). To obtain results consistent with a layer of current of the correct direction and approximate strength $I \cong 84$ A/km, we found it necessary to rotate $\mathbf{v}_{HT}$ by an angle of 7° around the + **j** axis (see Fig. 2), a deviation that is well outside the statistical error cone (±2°) but probably not much beyond the overall observational uncertainty (see below), to obtain a modified HT velocity $\tilde{\mathbf{v}}_{HT}$ = (GSE:–149, –207, 74) km/s. Moderate deviations of $\tilde{\mathbf{v}}_{HT}$ (by ± 2°, say) do not change the topological features of the field map.

To obtain a reasonable value of the component of $\tilde{\mathbf{v}}_{HT}$ along the magnetopause normal we also rotated the **n** vector by 3.3° around +**j** to obtain $\tilde{\mathbf{n}}$ = (GSE:0.8419, –0.5368, 0.0546). This rotation angle is at the edge of the statistical error cone for the minimum-variance direction, **k**. The resulting magnetopause speed, thickness, and average normal field component are $\tilde{\mathbf{v}}_{HT}\bullet\tilde{\mathbf{n}} = -10$ km/s, $h = (-\tilde{\mathbf{v}}_{HT}\bullet\tilde{\mathbf{n}})T_o = 660$ km (T_o = 66s = crossing duration), and $\langle\mathbf{B}\rangle\bullet\tilde{\mathbf{n}} = +0.32$ nT, respectively. Although these are reasonable values they are somewhat arbitrary: the observational results for this event do not permit a determination of the magnetopause speed and thickness.

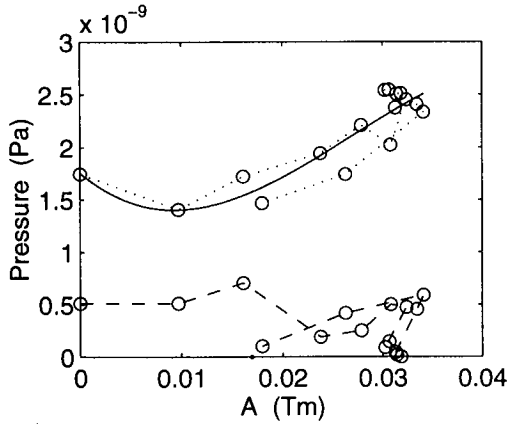

Figure 3. Pressures $B_z^2/2\mu_0$ (lower curve) and $(p + B_z^2/2\mu_0)$ (upper curves) as functions of the vector potential A. Solid curve represents cubic fit.

A second difficulty is the plasma pressure, p, during the crossing: the measured total pressure $(p+B^2/2\mu_0)$ has a substantial minimum in the middle of the current sheet, where a region of low magnetic field is encountered. During the event, the plasma instrument was in its half-sweep mode where the ion energy range sampled is reduced from 20 eV/q < E < 40 keV/q to 150 eV/q < E < 5.3 keV/q. Simulations of the instrument in this mode [Paschmann, private communication, 1996] indicate that, under typical magnetopause conditions, the pressure measured can be underestimated by as much as 40%; systematic directional errors of a few degrees of the measured velocities, and therefore of $\mathbf{v}_{HT}$, may also occur. Accordingly we have multiplied the measured pressure by a factor 1.3 which is sufficient to remove, on average, the defect in total pressure mentioned above. We have also used the measured pressure, $p_\perp$, transverse to **B** to represent p in our analysis but modest anisotropy ($p_\perp \sim 1.25 p_\parallel$) and non-gyrotropic effects (~10%) in the pressure tensor are in fact present. Generalization of our analysis to include these effects is important but nontrivial.

Next we looked for an invariant direction (z) such that the relation between $(p+B_z^2/2\mu_0)$ and A displays minimum scatter. We found this optimal direction of z to coincide approximately with the negative intermediate-variance axis (–**j** in Fig.2) which is also the approximate direction of the net magnetopause current during the crossing. The resulting relationship between $(p+B_z^2/2\mu_0)$ (as well as $B_z^2/2\mu_0$ alone) and A is shown in Fig.3. Although there is the suggestion of two branches, we chose to represent $(p+B_z^2/2\mu_0)$ by a single cubic curve representing the best least-squares fit to the data. This curve was then used to obtain the right-hand side of the GS equation. The value of the vector potential itself as a function of location (x) along the spacecraft trajectory is shown in Fig.4. It displays the broad maximum characteristic of a current layer having net current along the positive z direction. Use of $\mathbf{v}_{HT}$ rather than $\tilde{\mathbf{v}}_{HT}$ leads to a minimum instead. It also leads to a field map that is inconsistent with any simple interpretation of the event as a traversal of the magnetopause current layer.

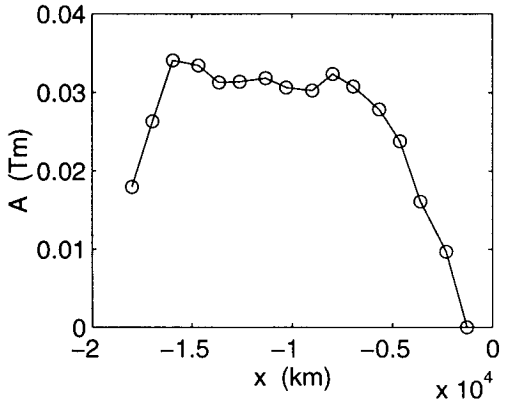

Figure 4. Vector potential, A, as a function of position, x, along the spacecraft trajectory.

The magnetic field map generated by our GS solver by use of band-limited interpolation of the measured data is shown in Fig.5a, with the distances along y expanded by a factor 10 to show details of the transverse field configuration. Also shown are small circles, indicating the locations along the spacecraft trajectory of the centers of the data samples (separated by 4.35s); attached to the circles are vectors showing the measured transverse **B** field. A plot of correct proportions is shown in Fig.5b where the true direction of the magnetopause normal is also indicated. A plot of this type is called a magnetic 'transect' of a portion of the magnetopause. Other types of transects can be readily produced by use of the field map. Since pressure p, density ρ, axial field component B_z, current density component j_z, and flow component v_z (if any) are all ideally functions of A, relief plots of these quantities are directly obtainable, at least in any portion of the xy plane connected by magnetic field lines to points on the spacecraft trajectory. A plot of the transverse current components j_x and j_y is similar to Fig. 5b, since $j_y/j_x = B_y/B_x$. Thus an essentially complete characterization of the MHD equilibrium is obtained.

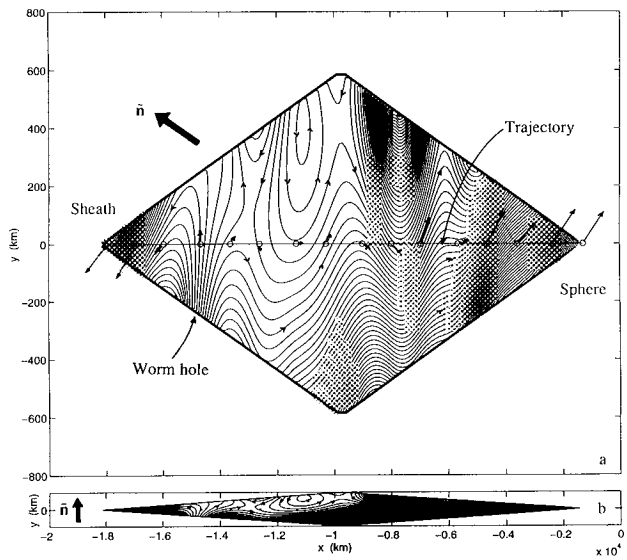

Figure 5. Magnetic transect of the magnetopause. (a) Map with y dimension expanded by factor 10. Spacecraft moves along horizontal rhombus diameter from right to left. Actual data sampling points are shown by small circles and measured transverse **B** vectors by arrows attached to them. (b) Map in actual proportions. Magnetopause normal vector, $\tilde{\mathbf{n}}$, is shown.

The magnetic transect in Fig.5 was calculated on the assumption that, throughout the map, $(p+B_z^2/2\mu_o)$ is the single-valued function of A shown by the solid curve in Fig.3. Extrapolation to positive A values outside the range calculated from (5) was provided by a simple straight-line extension of the cubic curve in Fig.3. This extension permitted inclusion of certain portions of the map that are not connected by field lines to the spacecraft trajectory; in those regions, the map, while plausible, is not unique. It should also be remembered that Fig. 5 represents a low-pass filtered version of the true map: the AMPTE/IRM sampling time, τ = 4.35s, imposes a wave-length (Nyquist) limit along x of $\lambda > 2\tau v_{ox} \cong 1700$ km.

Discussion

We have found that the qualitative features of the transect are consistent with overall expectations for a magnetopause crossing only when $\mathbf{v}_{HT}$ is modified to $\tilde{\mathbf{v}}_{HT}$. On the other hand, those features are insensitive to moderate changes in data filtering, moderate changes in the curve of $(p+B_z^2/2\mu_o)$ versus A in Fig.3, moderate changes in the pressure correction factor, above or below the chosen value of 1.3, and moderate deviations of the spacecraft trajectory from a straight line (these deviations from a simple constant velocity of the HT frame are estimated from the component perpendicular to **B** of the residual plasma velocity in the HT frame). The chosen value of normal velocity, $\tilde{\mathbf{v}}_{HT} \cdot \tilde{\mathbf{n}}$, affects only the magnetopause thickness. We now discuss the geophysical implications of the transect.

The magnetic-field behavior in the transect has expected as well as unexpected features. The appearance of a magnetic island, surrounded by two X-type nulls in the transverse field, as shown in the upper middle part of Fig. 5, is an expected feature of a TD-type current-layer structure, presumably caused by the tearing mode. The alternative would be the singular case of a null curve in the xy plane for the transverse field ($B_x = B_y = 0$). An unexpected feature is the presence, immediately to the left of the left X-type magnetic null of a field-line bundle that is oriented at a large angle to the magnetopause and that may possibly provide a direct magnetic connection across the magneto-pause, from the magnetosphere to the magnetosheath. Magnetically, the connection would be weak and dynamically insignificant because this part of the transect corresponds to the portion of the hodograms in Fig.2 where B_i, B_j and B_k are all relatively small (5 - 15 nT) and because the transverse dimension of the hole is small. Even so, the possibility that such weak-field connections, or 'worm holes' in the magnetopause, may serve as entry ports into the magnetosphere of plasma from the magnetosheath, or as exit ports for magnetospheric plasma, is of interest. Since the electric current lines in the xy plane are aligned with the magnetic field lines, an electric current connection across the magnetopause is also implied.

If a spacecraft were to travel along the straight-line trajectory marked in Fig.5a and measure the magnetic field **B** in our 2D model at the locations of the small circles, the hodogram pair constructed from those measured field vectors would look exactly as in Fig.2. In other words, a high-quality minimum-variance direction would be obtained with essentially zero average field component along that direction. These results would invite an interpretation in terms of a more or less 1D tangential discontinuity containing a layer of very weak field somewhere near its center. The current-layer structure we have recovered is significantly different from such a simple picture in that it contains a weak-field 2D worm hole crossing the magnetopause in addition to a weak-field layer containing magnetic islands. Our result therefore illustrates some of the dangers associated with the use of 1D models of the magnetopause structure. Although the plasma and field data for the event appear approximately consistent with the 2D model assumptions we have used, it is expected that, in reality, at least some 3D effects will be present as well. Thus the actual field structure, even in the low-pass filtered version studied here, is likely to be even more complicated.

Our new data analysis technique and its application to the magnetopause will be reported in further detail elsewhere. We emphasize that the method needs more testing, in particular by use of multi-spacecraft information, in order to establish its reliability and its limitations. Our analysis of the October 19, 1984, magnetopause crossing by AMPTE/IRM represents a first attempt to reconstruct a magnetic-field map from the GS equation. As such it is meant to be illustrative rather than optimal in all respects.

Field-aligned 2D flows are describable by a more complicated GS-type equation [*Sonnerup and Hau*, 1994]. Therefore, our method can be generalized, in principle, to deal with magnetopause reconnection events where a large field-aligned flow remains in the HT frame [e.g., *Sonnerup et al.*, 1990]. The method and its various extensions should also be of use in the study of 2D structures elsewhere in space, e.g., flux ropes in the geomagnetic tail and a variety of other field structures in the solar wind, magnetosheath or magnetosphere, convecting past an observing spacecraft.

Acknowledgments. We thank Dr. G. Paschmann for use of the AMPTE/IRM plasma and magnetic-field data and for valuable discussion. The research was supported by the National Aeronautics and Space Administration under grants NAGW-4023, NAG 5-3031 and NAG 5-2252, and by the National Science Foundation, Atmospheric Sciences Division, under grant ATM 9422918 to Dartmouth College.

References

Paschmann, G., I. Papamastorakis, W. Baumjohann, N. Sckopke, C.W. Carlson, B.U.Ö. Sonnerup and H. Lühr, The magnetopause for large magnetic shear: AMPTE/IRM observations, *J. Geophys. Res., 91*, 11,099, 1986.

Sonnerup, B.U.Ö., I. Papamastorakis, G. Paschmann, and H. Lühr, The magnetopause for large magnetic shear: Analysis of convection electric fields from AMPTE/IRM, *J. Geophys Res., 95*, 10,541, 1990.

Sonnerup, B.U.Ö., and L.-N. Hau, Vortex laws and field line invariants in polytropic field-aligned flow, *J. Geophys. Res., 99*, 143, 1994.

Sturrock, P., *Plasma Physics, An Introduction to the Theory of Astrophysical, Geophysical and Laboratory Plasmas*, Cambridge Univ. Press, p. 209, Cambridge, 1994.

B.U.Ö. Sonnerup and M. Guo, Thayer School of Engineering, Dartmouth College, 8000 Cummings Hall, Hanover, NH
(e-mail: sonnerup@dartmouth.edu)

(Received August 26, 1996; revised October 28, 1996;
accepted November 11, 1996.)